

Accepted Manuscript

Quarterly Journal of Engineering Geology and Hydrogeology

The thermal properties of the Mercia Mudstone Group

Dan Parkes, Jon Busby, Simon J. Kemp, Estelle Petitclerc & Ian Mounteney

DOI: <https://doi.org/10.1144/qjegh2020-098>

To access the most recent version of this article, please click the DOI URL in the line above.

Received 20 May 2020

Revised 9 September 2020

Accepted 9 September 2020

© 2020 UKRI. The British Geological Survey. Published by The Geological Society of London. All rights reserved. For permissions: <http://www.geolsoc.org.uk/permissions>. Publishing disclaimer: www.geolsoc.org.uk/pub_ethics

When citing this article please include the DOI provided above.

Manuscript version: Accepted Manuscript

This is a PDF of an unedited manuscript that has been accepted for publication. The manuscript will undergo copyediting, typesetting and correction before it is published in its final form. Please note that during the production process errors may be discovered which could affect the content, and all legal disclaimers that apply to the journal pertain.

Although reasonable efforts have been made to obtain all necessary permissions from third parties to include their copyrighted content within this article, their full citation and copyright line may not be present in this Accepted Manuscript version. Before using any content from this article, please refer to the Version of Record once published for full citation and copyright details, as permissions may be required.

The thermal properties of the Mercia Mudstone Group

Dan Parkes¹, Jon Busby¹, Simon J. Kemp¹, Estelle Petitclerc² and Ian Mounteney¹

¹ British Geological Survey, Keyworth, Nottingham, NG12 5GG, UK

² Royal Belgian Institute of Natural Sciences, Geological Survey of Belgium, Rue Jenner, 13, 1000-Brussels

Email jpbu@bgs.ac.uk

Abstract

The Mercia Mudstone Group (MMG) crops-out extensively across England and Wales and its thermal properties are required for the design of infrastructure such as ground source heating and cooling schemes and electrical cable conduits. Data from the literature and new data from a borehole core have been compiled to generate an updated range of thermal conductivities related to rock type and the lithostratigraphy. These indicate a total range in saturated vertical thermal conductivity of 1.67–3.24 W m⁻¹ K⁻¹, comprising 1.67–2.81 W m⁻¹ K⁻¹ for mudstones, 2.12–2.41 W m⁻¹ K⁻¹ for siltstones and 2.3–3.24 W m⁻¹ K⁻¹ for sandstones. These data are all from measurements on samples and there will be uncertainty when considering the thermal properties of the rock mass due to micro and macro structural features. Geometric mean modelling of thermal conductivity based on mineralogy has overestimated the thermal conductivity. Correction factors for the modelled thermal conductivities have been calculated to enable a first estimate of MMG thermal conductivities when only mineralogical data are available. Measured thermal diffusivities from the borehole core were in the range of 0.63–3.07 x10⁻⁶ m²s⁻¹ and are the first measured, thermal diffusivities to be reported for the MMG.

The Mercia Mudstone Group (MMG) crops-out extensively across England and Wales (see Fig 1). From the south, it extends from east Devon, Somerset, the Bristol area and south

Wales to the Gloucester and Worcester regions. Northwards, the outcrop broadens to underlie much of Warwickshire, Staffordshire and Leicestershire. To the east of the Pennines, it extends northwards through Nottinghamshire and Yorkshire and reaches the North Sea coast near Hartlepool. To the west of the Pennines, it underlies northern Shropshire, Cheshire and Merseyside, the Formby and Fylde peninsulas and farthest north, crops-out near Carlisle. Many towns and cities are underlain by the MMG including, Cardiff, Bristol, Worcester, southeast Birmingham, Leicester, Derby, Nottingham, Newark-on-Trent, Southport and Blackpool, where a knowledge of the thermal properties of the MMG is required for the design of infrastructure such as ground source heating and cooling schemes, underground thermal energy storage (UTES), tunnels, and electrical cable conduits.

The purpose of this technical note is to provide an up-to-date account of the thermal properties of the MMG onshore UK. After an introduction to the lithostratigraphy of the MMG, existing thermal property data are reviewed followed by a detailed analysis of core from a recently completed borehole in the East Midlands. These new data provide calibration for estimates of thermal conductivity from mineralogical analyses, and finally all the data are combined to provide a 'best estimate' of MMG thermal properties.

It should be noted that the term mudstone implies a very-fine-grained sedimentary rock in which the main constituents have grain sizes less than 63 μm , although the British Geological Survey suggest a grain size of less than 32 μm (Merriman et al., 2003). The primary components are clay minerals and quartz. However, the MMG has varied lithologies including some arenaceous units of silt and sand sized grains and overall it is probably more representative of a silty mudstone.

The Mercia Mudstone Group

A revision of the lithostratigraphic nomenclature for the MMG was published by Howard et al. (2008) and replaced that of Warrington et al. (1980). This new nomenclature is referred to as

the revised lithostratigraphy and a simplified description is given here. This simplified description provides the geological framework for the thermal properties and is intended to be used without expert geological knowledge. The onshore MMG of England and Wales comprises red, and less commonly green and grey mudstone and siltstone. Halite deposits occur in Dorset, Somerset, Worcestershire, Staffordshire, Cheshire, west Lancashire and south Cumbria, and east and north Yorkshire. Sulphate deposits of gypsum and anhydrite, and sandstone beds are common at some stratigraphic levels, but are a minor constituent of the Group. Table 1 presents the formation nomenclature for the MMG with a brief lithological description taken from the British Geological Survey's (BGS) Lexicon of Named Rock Units (<https://www.bgs.ac.uk/lexicon/?src=topNav>). In many regions, formations are sub-divided into members, many of which correspond to formations in the replaced lithostratigraphy of Warrington et al. (1980), although these are not referred to here. Howard et al. (2008) give the full lithostratigraphy for the ten regions shown in Figure 1. Rock types referred to in Table 1 and subsequent tables are explained in Table 2.

Laboratory testing for thermal conductivity (and diffusivity) of a sample depends on mineralogy, porosity, pore filling fluid and micro structure. This may differ from the thermal conductivity of the rock mass where macro structures (e.g., bedding, fractures, etc.) also have an influence. A thermal response test (TRT) conducted in closed loop boreholes drilled for the installation of ground source heat pumps measures an apparent thermal conductivity for the rock mass. A TRT can be affected by advective heat transfer due to groundwater flow and hence this apparent thermal conductivity may differ from the intrinsic thermal conductivity of a sample or the rock mass. Thermal conductivity is a tensor and the value measured horizontally will often differ to that vertically due to anisotropy within the rock. This often occurs in layered sedimentary rocks especially those comprised of platy minerals such as clays. Bloomer (1981) in measurements of thermal conductivity of United Kingdom mudrocks found the thermal conductivity measured parallel to bedding was 1.19 – 2.17 times higher than that measured perpendicular to bedding and noted that the anisotropy was

less for the siltier facies. Large infrastructure schemes (e.g., transit tunnels, ground source heating and cooling for commercial and public buildings) will require site specific thermal properties that can only be derived from an onsite test such as a TRT. Databased thermal properties derived from sample testing, as presented here, are suitable for smaller infrastructure (e.g., domestic ground source heating and cooling) where the design can include some tolerance due to the lack of site specific values.

There is little thermal property data for the MMG in the literature. The Microgeneration Installation Standard for ground source heat pumps (MIS 3005 v5, 2017) lists a range of thermal conductivity for Marl of 1.5-3.5 W m⁻¹ K⁻¹ with a recommended value of 2.1 W m⁻¹ K⁻¹. Quoted thermal conductivities for the MMG are 2.28 ± 0.33 W m⁻¹ K⁻¹ (Bloomer, 1981), 1.88 ± 0.03 W m⁻¹ K⁻¹ (Rollin, 1987) and 1.49–2.58 W m⁻¹ K⁻¹ (Banks et al., 2013) from in-situ TRT. Given the lithological variation within the MMG, a mean value for the bulk MMG is unlikely to be representative of a site specific effective thermal conductivity. The mean values quoted by Bloomer (1981) and Rollin (1987) are based on 41 and 225 laboratory measurements on samples respectively and assign a rock type of mudstone although a mix of lithologies are included. These data were collected as part of the 'Investigation of the geothermal energy of the UK' programme (Downing and Gray, 1986) and are re-examined here. The data were collected for heat flow studies where the thermal conductivity perpendicular to bedding is required. Measurements were made either from core in a divided bar apparatus, where the natural moisture level was preserved, from rock chippings placed in a pill box placed in the divided bar apparatus or with a needle probe. In the case of the pill box measurements, corrections were applied to generate the bulk rock thermal conductivity, but the random nature of the packing of the chippings in the pill box results in an averaged parallel/perpendicular to bedding thermal conductivity (Wheildon et al., 1985). Neither Bloomer (1981) nor Rollin (1987) give a breakdown on the numbers of each type of measurement in their mean values. However, the data re-examined here are most likely the same as used by Rollin (1987) and of 220 measurements only 20 (9%) were by the pill box

method. Hence, it is reasonable to assume that the majority were measurements of thermal conductivity perpendicular to bedding. The measurements of Banks et al. (2013) from TRT tests where heat flows radially from a borehole will be representative of horizontal thermal conductivity under field saturation conditions.

The individual measurements have been grouped by rock type, assignment to the revised lithostratigraphy (Howard et al., 2008) and provenance and the results are shown in Table 3. Measured thermal conductivities from the Cleethorpes geothermal borehole for the East Midlands Shelf (north) are uniformly high and as noted by Busby (2018) there appears to be a systematic error in the thermal conductivities from this borehole, and hence they have been excluded. All of these data are thermal conductivities perpendicular to bedding with the exception of the bulk MMG value ($1.95 \text{ W m}^{-1} \text{ K}^{-1}$) in the Wessex Basin, which was from pill box measurements on chippings from the Marchwood borehole. The data in Table 3 show a range of values from $1.71\text{--}4.43 \text{ W m}^{-1} \text{ K}^{-1}$ with representative thermal conductivities for mudstone of $2.10 \text{ W m}^{-1} \text{ K}^{-1}$, silty mudstone $1.87 \text{ W m}^{-1} \text{ K}^{-1}$, siltstone $2.24 \text{ W m}^{-1} \text{ K}^{-1}$ and sandstone $3.31 \text{ W m}^{-1} \text{ K}^{-1}$. There are no reported measurements of thermal diffusivity.

GeoEnergy Test Bed borehole

The British Geological Survey and the University of Nottingham have established a GeoEnergy Test Bed (GTB) research site to monitor CO_2 migration pathways in the shallow subsurface with advanced sensor technologies (Vincent et al., 2019). The GTB is located at the University of Nottingham's Sutton Bonington campus to the southwest of Nottingham (Longitude $-1^\circ 15' 1.46''$, Latitude $52^\circ 49' 51.44''$; British National Grid 450600E, 326200N). There are eleven boreholes on site, one of which was cored to its full depth of 282 m. This borehole penetrates a section of the East Midlands MMG comprising, the Arden Sandstone Formation, the Sidmouth Mudstone Formation and the Tarporley Siltstone Formation. It therefore provides an opportunity to study in detail a section of the MMG and relate its thermal properties to structure and mineralogy. Twenty samples taken from the borehole

core through this section were described and analysed to determine porosity, mineralogy and laboratory thermal properties.

Rock description

The upper two samples, SSK109105 and SSK109102, are from the Arden Sandstone Formation (see Table 4). The upper sample is a variably coloured, friable sandstone with near abundant, horizontal gypsum veining, whilst the lower sample is a light brown to red brown sandy mudstone with hairline horizontal gypsum veins throughout. The majority of the cored sequence (14 samples) is from the Sidmouth Mudstone Formation. The samples from 21.7–46.0 m depth are brown to light brown and pale grey mudstones with near horizontal to horizontal gypsum veining throughout. The samples from 54.6–65.4 m depth are pale grey bleached fine sandstone with some poorly defined horizontal, fine paler bands and light red brown to light grey green (mottled) silty very fine to fine sandstones. Red brown and pale brown sandy mudstones occur between 67.8–77.1 m depth and the sample at 85.6–85.7 m depth is a red brown mudstone with pale grey brown coloured wisps that show clear laminated structure. The remainder of the Sidmouth Mudstone Formation is arenaceous with silty very fine sandstones and massive very silty, clayey very fine-grained sandstone with gypsum veining increasing towards the base of the Formation. The upper sample in the Tarporley Siltstone Formation (131.9–132.0 m depth) is a massive red brown very silty very fine sandstone. The sample from 140.4–140.6 m depth interval is a more variable sample comprising muddy clasts in a mud clast rich bed with no gypsum veining. The final two samples at the base of the cored section comprise red-brown and grey-brown silty very fine sandstone and a mottled grey-green to red-brown-grey fine siltstone with some well-developed horizontal laminations, possibly current ripples.

Porosity estimations

The samples were saturated with water under vacuum before drying at 100 °C for 16 hours. The weight difference before and after drying was used to estimate the effective porosity. Such estimates will have an element of error due to water adsorbed onto grain or clay mineral surfaces, particularly for the clay rich samples. Additionally, the rocks have a fine grain size, are heavily compacted and have a high clay content which means that the diameter of pore throats, which connect pores are likely to be small and also infilled with impermeable clay material, limiting the effectiveness of the saturating and drying process.

X-ray diffraction analysis

The mineralogy of the samples was determined using a combination of whole-rock and <2 µm X-ray diffraction (XRD) analyses.

Sample preparation

The core samples were dried at 55°C overnight and jaw-crushed. Half of the jaw-crushed material was representatively subsampled and ball-milled for whole-rock XRD analyses.

In order to provide a finer and uniform particle-size for powder XRD analysis, a portion of the ball-milled sample was micronised under distilled water for 10 minutes with 10% corundum and dried at 55°C. The samples were then spray-dried following the method and apparatus described by Hillier (1999). The spray-dried material was then front-loaded into a standard stainless steel sample holder for analysis.

To separate a fine fraction for clay mineral XRD analysis, further portions of the jaw-crushed material were dispersed in distilled water using a reciprocal shaker combined with ultrasound treatment and then wet-sieved on 63 µm mesh. The coarse (>63 µm) material was collected and dried in an oven at 55 °C ('sand'). The <63 µm material was placed in a measuring cylinder with a few drops of 0.1M Calgon solution to prevent clay flocculation and shaken. The suspension was left to settle and after a time period determined from Stokes' Law, a nominal <2 µm fraction was removed to a stock beaker. The cylinders were then topped-up

with distilled water, shaken, and the suspensions allowed to stand for a similar time period before a further $<2\ \mu\text{m}$ fraction was removed and added to the stock beaker. The process was repeated for a third extraction before the $<2\ \mu\text{m}$ material was then dried at 55°C and stored in glass vials ('clay'). The remaining $2\text{-}63\ \mu\text{m}$ was also dried at 55°C and stored in glass vials ('silt').

Approximately 100 mg of the dried $<2\ \mu\text{m}$ material was then re-suspended in a minimum of distilled water and pipetted onto a ceramic tile in a vacuum apparatus to produce an oriented mount. The mounts were Ca-saturated using $0.1\text{M}\ \text{CaCl}_2\cdot 6\text{H}_2\text{O}$ solution, washed twice to remove excess reagent and allowed to air-dry overnight.

The preparation of $<2\ \mu\text{m}$ material for XRD analysis therefore also provided a crude particle-size analysis for the samples. However, these PSD data should be regarded with caution since the samples were not fully disaggregated and therefore the proportions of 'sand'- and 'silt'-grade material are almost certainly over-estimates and the quantity of 'clay'-grade material is therefore underestimated.

Analysis

XRD analyses were carried out using a PANalytical X'Pert Pro series diffractometer equipped with a cobalt-target tube, X'Celerator detector and operated at 45kV and 40mA .

The spray-dried powder mounts were scanned from $4.5\text{-}85^\circ 2\theta$ at $2.06^\circ 2\theta/\text{minute}$. Diffraction data were analysed using PANalytical X'Pert HighScore Plus version 4.8 software coupled to the latest version of the International Centre for Diffraction Data (ICDD) database.

The $<2\ \mu\text{m}$ oriented mounts were scanned from $2\text{-}40^\circ 2\theta$ at $1.02^\circ 2\theta/\text{minute}$ after air-drying, after glycol-solvation and after heating to 550°C for 2 hours.

Whole-rock quantification

Following identification of the mineral species present in the sample, phase quantification was achieved using the Rietveld refinement technique (e.g. Snyder & Bish, 1989) using

PANalytical HighScore Plus software. Errors for the quoted mineral concentrations are typically $\pm 1\%$ for concentrations >50 wt%, $\pm 5\%$ for concentrations 10–50 wt%, $\pm 10\%$ for concentrations <10 wt% (e.g. Kemp et al., 2016a). Where a phase was detected but its concentration was indicated to be below 0.5%, it is assigned a value of $<0.5\%$, since the error associated with quantification at such low levels becomes too large.

XRD-profile modelling

In order to gain further information about the nature of the clay minerals present in the sample, modelling of the XRD profiles was carried out using Newmod II™ (Reynolds & Reynolds, 2013) software following the methodology summarised by Kemp *et al.* (2016b). Modelling was also used to assess the relative proportions of clay minerals present in the <2 μm fraction by comparison of sample XRD traces with Newmod II™ modelled profiles following the method outlined in Moore & Reynolds (1997).

Thermal properties measurements

Laboratory measurements of thermal conductivity and diffusivity of the GTB samples were undertaken by the Geological Survey of Belgium (GSB). At each of the twenty sampling points down the GTB core, two samples were taken. One half of the sample was used for the XRD analysis, whilst the second was cut into a smooth sided square block of dimensions 40 x 40 x 10 mm. Due to the sampling technique the samples were not orientated and therefore it is not known if the thermal properties measurements were parallel or perpendicular to bedding. The thermal properties measurements were made in Belgium with the high-resolution optical Thermal Conductivity Scanning method (Popov, 1999; 2012). It is a high precision non-contact measurement that optically scans the sample's surface with a focussed, mobile and continuously operated heat source in combination with two infrared temperature sensors. After warming up the instrument, the sensors were calibrated with a reference sample. The measurements were made on a 2 cm wide black mark made on the plane surface of each sample. All the measurements were repeated three times from which

mean values were calculated. The device operates in two modes; thermal conductivity alone, or a combined mode of thermal conductivity and thermal diffusivity. Measurements were made initially on unsaturated samples and then repeated after saturation in a vacuum desiccator by demineralized water for 5 to 10 days. The results quoted here are only for saturated samples and the thermal conductivity results are from the thermal 'conductivity alone' mode, whilst the thermal diffusivity results are from the combined mode. Sample SSK109089 was fractured and broken resulting in inconsistent results, especially between the unsaturated and saturated states, and so has been discounted. The specific heat capacity by mass was calculated as the saturated density was measured during the porosity measurement. It is given by,

$$S_c = \frac{\lambda}{\alpha\rho}$$

where S_c is the specific heat by mass ($\text{J K}^{-1} \text{kg}^{-1}$), λ is thermal conductivity ($\text{W m}^{-1} \text{K}^{-1}$), ρ is the saturated density (kg m^{-3}) and α is the thermal diffusivity ($\text{m}^2 \text{s}^{-1}$). The specific heat capacity by volume has also been calculated, as it is the product of the specific heat by mass and the density.

Results of the GTB core analyses

Porosity and XRD mineralogical results are summarised in Table 4. Mineral contents were measured as weight percentages of the sample, converted to volume percentages of the sample and finally converted to volume percentages of the rock, taking into consideration the effective porosity. The proportions of illite were measured in the $<2 \mu\text{m}$ material analyses where illite is the dominant clay mineral. Quartz is the most abundant mineral followed by dolomite and gypsum. Measured thermal conductivities, thermal diffusivities, saturated densities and derived specific heats are given in Table 5. Thermal conductivity has a range from $1.64\text{--}5.6 \text{ W m}^{-1} \text{K}^{-1}$. The highest thermal conductivities correlate with samples with high percentages of high thermal conductivity minerals and/or low porosities. A high porosity will

lower the thermal conductivity as the pore space is filled by low thermal conductivity water. Sample SSK109082, which has the highest thermal conductivity of $5.6 \text{ W m}^{-1} \text{ K}^{-1}$, contains 59.7% quartz and 22.1% anhydrite (mineral thermal conductivities of 7.69 and $4.76 \text{ W m}^{-1} \text{ K}^{-1}$ respectively) and a low porosity of 4.2%. Sample SSK109100 has the second highest thermal conductivity of $4.14 \text{ W m}^{-1} \text{ K}^{-1}$ and has the highest quartz content of 81.1%, but a higher porosity of 11.6%. The Arden Sandstone samples (SSK109105 and SSK109102) both have relatively low thermal conductivities corresponding with low quartz content, high gypsum content (thermal conductivity $2.9 \text{ W m}^{-1} \text{ K}^{-1}$) and high porosities. Secondary mineralisation in the form of veins and nodules is common in the MMG and where it occurs it could have a significant influence on the thermal conductivity. Gypsum is also likely to occur as a cement, connecting/bridging the higher conducting quartz grains, which would have the overall effect of lowering the thermal conductivity of the rock.

From the repeated measurements on the GTB core samples there is an overall measurement error of $\pm 2\%$ in thermal conductivity and $\pm 6\%$ in thermal diffusivity. Uncertainty will be greater due to micro structural features such as bedding and when translating measured sample values to the rock mass where macro structural features may have an effect.

For the sizing of a GSHP closed loop borehole, it is the average thermal conductivity of the strata over the length of the borehole that is required. For the GTB core, it has been assumed that each sample is representative of an equal thickness layer within each Formation. This translates to layer thicknesses of 4.5 m within the Arden Sandstone, 7.9 m within the Sidmouth Mudstone and 7 m within the Tarporley Siltstone. Since heat will be flowing horizontally into the borehole an arithmetic mean, weighted by the layer thicknesses, has been calculated as $2.63 \text{ W m}^{-1} \text{ K}^{-1}$. This is higher than might be expected for a rock referred to as a mudstone, but reflects the arenaceous nature of the sequence in the GTB core. From four TRT measurements, Banks et al. (2013) quote an upper MMG thermal conductivity of $2.58 \text{ W m}^{-1} \text{ K}^{-1}$, a value compatible with that from the GTB core.

Figure 2 shows a plot of increasing thermal conductivity with decreasing effective porosity, which displays a non-linear relationship. The thermal diffusivities show a range of 0.63 - 3.07 $\times 10^{-6} \text{ m}^2\text{s}^{-1}$. There are no published data on measured thermal diffusivities of the MMG, but these values are comparable to those reported by Labus and Labus (2018) on fine grained sedimentary rocks. The specific heats by mass range from 563 – 1426 $\text{J K}^{-1} \text{ kg}^{-1}$ and the specific heats by volume range from 1.48 – 3.19 $\text{MJ m}^{-3} \text{ K}^{-1}$.

Estimations of thermal conductivity from mineral content

The number of thermal conductivity determinations can be increased by applying a modelling approach when the mineral content of the rock is known. This has been applied to two sets of MMG samples reported in the literature by Kemp and Hards (1999) and Armitage et al. (2013). However, because the GTB site has yielded both laboratory determinations of thermal conductivity and mineral content, the modelling procedure has been tested for its effectiveness for Mercia Mudstone before being applied to the data of Kemp and Hards (1999) and Armitage et al. (2013).

The modelling was based on multi-component mixture models, as summarised by Clauser (2006). Due to their well-defined compositions, the thermal conductivities of individual minerals show a much smaller variance than rocks and can be combined with the thermal conductivities of the saturating fluids to estimate the thermal conductivity of the rock. Fuchs et al. (2013) examined the goodness-of-fit between measured and modelled thermal conductivities for 1147 samples of sedimentary rocks (sandstone, mudstone, limestone and dolomite). They compared five mixture models comprising the geometric mean, the arithmetic mean, the harmonic mean, the Hashin and Shtrikman mean and the effective-medium theory mean. They only considered a two-component system comprising rock matrix and pores, but concluded that the geometric mean gave the best results. Hence, the geometric mean model has been applied here. The geometric mean thermal conductivity of

an n-component system is the product of the thermal conductivity of each component raised to the power of its volume fractional component, i.e.

$$\lambda_b = \prod_{i=1}^n \lambda_i^{\varphi_i}$$

where λ_b is the mean bulk thermal conductivity, λ_i is the thermal conductivity of the *i*th component and φ_i is the volume fractional proportion of the *i*th component.

The thermal conductivities of the model components are listed in Table 6. It has been assumed that the samples are fully saturated with water. The calculated thermal conductivities are shown in Table 7.

Also listed in Table 7 are the measured thermal conductivities and the deviation between the measured and calculated thermal conductivities, and Figure 3 is a plot of measured versus calculated thermal conductivity. Except for one sample, the geometric mean calculated thermal conductivities are higher than the measured values indicating an over estimation of mudstone thermal conductivity with the geometric mean model, an observation noted by Midttømme et al., 1998. A simple correction factor has been calculated as the average absolute deviation between the calculated and measured thermal conductivities. Correction factors for the mudstone and sandstone lithotypes have been calculated separately, where the lithotype is based on the rock description. The correction factors are $0.63 \text{ W m}^{-1} \text{ K}^{-1}$ for mudstone and $0.96 \text{ W m}^{-1} \text{ K}^{-1}$ for sandstone and these values were subtracted from the calculated thermal conductivities. The corrected values are listed in Table 7 and shown in Figure 3.

Kemp and Hards (1999) report the results of mineralogical, petrological and surface area analyses from five samples taken from shallow boreholes at Northgates, Leicester. The samples were described as predominantly mudstone with some silty mudstone and siltstone. The samples are from the Sidmouth Mudstone Formation and, from the clay mineral assemblages, are representative of an interval that spans the junction between the Edwalton

and Cropwell Bishop members. Kemp and Hards (1999) did not measure effective porosity and so the average value of the GTB mudstone samples (21%) has been used. The mineral compositions of the samples are shown in Table 8. Armitage et al. (2013) studied six samples from depths between 300 and 310 m from the Willow Farm borehole in the East Midlands near Nottingham (Longitude $-0^{\circ}, 52' 52.00''$ Latitude $52^{\circ}, 51' 27.23''$; British National Grid 475434E, 329483N). The samples vary from muddy siltstones to silty to very fine-grained sandstones and are also from the Sidmouth Mudstone Formation. The mineral compositions are also listed in Table 8. Thermal conductivities for these 11 samples have been calculated with the geometric mean model and corrected using the correction factors estimated above and the results are listed in Table 9. The range of the corrected geometric mean thermal conductivity values is $1.62 \text{ W m}^{-1} \text{ K}^{-1}$ (silty mudstone) to $3.01 \text{ W m}^{-1} \text{ K}^{-1}$ (sandstone).

Discussion

The measured thermal conductivities from the GTB core have been incorporated with the data in Table 3 to create a revised set of thermal conductivities for the East Midlands shelf (south) MMG, and this is shown in Table 10. From a consideration of all the measured data (Tables 3 and 10), there is a range in thermal conductivity of $1.67\text{--}3.24 \text{ W m}^{-1} \text{ K}^{-1}$ for the MMG. The lower values are for the mudstones, $1.67\text{--}2.81 \text{ W m}^{-1} \text{ K}^{-1}$. The siltstones range from $2.12\text{--}2.41 \text{ W m}^{-1} \text{ K}^{-1}$ and the sandstones from $2.3\text{--}3.24 \text{ W m}^{-1} \text{ K}^{-1}$.

The uncorrected thermal conductivities calculated from the mineral content are uniformly higher than the measured values for the GTB core. Midttømme et al., 1998 in a study of mudstones noted that the grain size distribution may be a factor in the determination of thermal conductivity. Low measured thermal conductivities correlated with rocks with a high clay fraction, whilst rocks with a high sand fraction were associated with high thermal conductivities. Figure 4 is a plot of the clay fraction ($<2 \mu\text{m}$) and the sand fraction ($>63 \mu\text{m}$) of the GTB samples plotted against the measured thermal conductivity. Trends of higher

measured thermal conductivity associated with a higher sand fraction and lower measured thermal conductivity associated with a higher clay fraction are apparent, suggesting that a model that does not take into account particle size fractions may not be suitable for predicting the thermal conductivity of the MMG.

There are other considerations for the mismatch between measured and modelled thermal conductivity. Firstly, the model does not take into account anisotropy. Mudstones often display a different thermal conductivity parallel and perpendicular to bedding (Bloomer, 1981). In the measurements from the GTB core no account was taken of anisotropy and so it is not possible to quantify the effect of anisotropy on the modelling. Secondly, the model only considers porosity that is assumed to be saturated, whilst for mudstones there may be water adsorbed onto grain or clay mineral surfaces that is not accounted for in the model.

From the GTB results, correction factors for the mudstone and sandstone lithotypes were applied to the calculations from Kemp and Hards (1999) and Armitage et al. (2013). These data have not been incorporated in the summary in Table 10 due to the limitations in the geometric mean model. However, the corrected thermal conductivities do fall within the ranges observed for measured values. Hence, if only mineralogical information is available, calculated thermal conductivities based on corrected geometric mean modelling may be valid for a first estimate of MMG thermal conductivity.

Conclusions

Previous publications that have included the thermal properties of the MMG have treated the Group as a single rock type and generated an average thermal conductivity from measurements on multiple lithologies. Data from the literature and new thermal conductivity and diffusivity measurements on a cored section of the MMG from the GTB borehole have been combined to generate revised thermal properties for the MMG. These indicate a total range in saturated vertical thermal conductivity of 1.67–3.24 W m⁻¹ K⁻¹, comprising 1.67–2.81 W m⁻¹ K⁻¹ for mudstones, 2.12–2.41 W m⁻¹ K⁻¹ for siltstones and 2.30–3.24 W m⁻¹ K⁻¹ for

sandstones. There is still limited availability of data and it is therefore not possible to draw conclusions about the variation of MMG thermal properties between the regions. However, the measured thermal diffusivities, ranging from $0.63 - 3.07 \times 10^{-6} \text{ m}^2 \text{ s}^{-1}$, are amongst the first published values for the MMG. These data are all from measurements on samples and there will be uncertainty when considering the thermal properties of the rock mass due to micro and macro structural features. However, these data will improve the design of smaller infrastructure, such as domestic scale ground source heat and cooling, where it is not possible to obtain site specific thermal properties. Larger infrastructure schemes, where site specific properties are required, should include a TRT in the design process.

The total number of estimations of thermal conductivity has been increased with geometric mean modelling based on mineralogy. Comparison with the measured thermal conductivities from the GTB core indicates that the modelled data are overestimated. Correction factors of $0.63 \text{ W m}^{-1} \text{ K}^{-1}$ for mudstone lithotypes and $0.96 \text{ W m}^{-1} \text{ K}^{-1}$ for sandstone lithotypes can be applied to enable a first estimate of MMG thermal conductivities when only mineralogical data are available.

Acknowledgements

Oliver Wakefield is thanked for his initial logging of the core from the GTB borehole. Dan Parkes, Jon Busby, Simon Kemp and Ian Mounteney publish with the permission of the Executive Director, British Geological Survey (UKRI).

Funding

The research was funded by the British Geological Survey (UKRI).

References

Armitage, P.J., Worden, R.H., Faulkner, D.R., Aplin, A.C., Butcher, A.R. & Espie, A.A. 2013. Mercia Mudstone Formation caprock to carbon capture and storage sites: petrology and petrophysical characteristics. *Journal of the Geological Society, London*, **170**, 119–132. doi: 10.1144/jgs2012-049.

Banks, D., Withers, J.G., Cashmore, G. & Dimelow, C. 2013. An overview of the results of 61 in situ thermal response tests in the UK. *Quarterly Journal of Engineering Geology and Hydrogeology*, **46**, 281-291.

Bloomer, J.R. 1981. Thermal conductivities of mudrocks in the United Kingdom. *Quarterly Journal of Engineering Geology*, **14**, 357-362.

Brigaud, F. & Vasseur, G. 1989. Mineralogy, porosity and fluid control on thermal conductivity of sedimentary rocks. *Geophysical Journal*, **98**, 525–542.

Busby, J. 2018. A modelling study of the variation of thermal conductivity of the English Chalk. *Quarterly Journal of Engineering Geology and Hydrogeology*, **51**, 417-423.

<https://doi.org/10.1144/qjegh2017-127>

Clauser, C. 2006. Geothermal energy. In: Heinloth, K. (ed.) *Landolt-Börnstein, Group VIII: 'Advanced Materials and Technologies', Vol. 3 'Energy Technologies', Subvol. C 'Renewable Energies'*. Springer, Heidelberg, 480–595.

Clauser, C. & Huenges, E. 1995. Thermal conductivity of rocks and minerals. In: Ahrens, T.J. (ed.) *Rock Physics & Phase Relations: A Handbook of Physical Properties*. Geophysical Union, 105–126.

Downing, R.A. & Gray, D.A. 1986. Geothermal resources of the United Kingdom. *Journal of the Geological Society, London*, **143**, 499-507.

Fuchs, S., Schütz, F., Förster, H.-J. & Förster, A. 2013. Evaluation of common mixing models for calculating bulk thermal conductivity of sedimentary rocks: Correction charts and new conversion equations. *Geothermics*, **47**, 40-52.

Hillier, S. 1999. Use of an air-brush to spray dry samples for X-ray powder diffraction. *Clay Minerals*, **34**, 127–135.

Horai, K. 1971. Thermal conductivity of rock forming minerals. *Journal of Geophysical Research*, **76**, 1278–1308.

Howard, A.S., Warrington, G., Ambrose, K. & Rees, J.G. 2008. A formational framework for the Mercia Mudstone Group (Triassic) of England and Wales. *British Geological Survey Research Report*, RR/08/04.

Kemp, S.J. & Hards, V.L. 1999. The mineralogy and microtextures of samples of the Mercia Mudstone Group from Northgates, Leicester. *British Geological Survey Technical Report* WG/99/25C.

Kemp, S.J., Smith, F.W., Wagner, D., Mounteney, I., Bell, C.P. Milne, C.J., Gowing, C.J.B. & Pottas, T.L. 2016a. An improved approach to characterise potash-bearing evaporite deposits, evidenced in North Yorkshire, UK. *Economic Geology*, **111**(3), 719–742.

Kemp, S.J., Ellis, M.A., Mounteney, I. & Kender, S. 2016b. Palaeoclimatic implications of high-resolution clay mineral assemblages preceding and across the onset of the Palaeocene-Eocene thermal maximum, North Sea Basin. *Clay Minerals*, **51**, 793-813.

Labus, M. & Labus, K. 2018. Thermal conductivity and diffusivity of fine-grained sedimentary rocks. *Journal of Thermal Analysis and Calorimetry*, **132**, 1669-1676.

<https://doi.org/10.1007/s10973-018-7090-5>

Merriman, R.J., Highley, D.E. & Cameron, D.G. 2003. Definition and characteristics of very-fine grained sedimentary rocks: clay, mudstone, shale and slate. *British Geological Survey Commissioned Report* CR/03/281N. 20 pp.

Midttømme, K., Roaldset, E. & Aagaard, P. 1998. Thermal conductivity of selected claystones and mudstones from England. *Clay Minerals*, **33**, 131–145.

MIS 3005 v5, 2017. *Microgeneration Installation Standard: MIS 3005. Requirements for MCS contractors undertaking the supply, design, installation, set to work, commissioning and handover of microgeneration heat pump systems Issue 5.0*. Department of Energy and Climate Change. <https://mcscertified.com/wp-content/uploads/2019/08/MIS-3005.pdf>

Moore, D.M. & Reynolds, R.C. 1997. X-Ray Diffraction and the Identification and Analysis of Clay Minerals, Second Edition. Oxford University Press, New York.

Ozbek, H. & Phillips, S. 1979. *Thermal conductivity of aqueous NaCl solutions from 20 °C to 330 °C*. University of California, LBL Report No. 9086, Berkeley, USA.

Popov, Y., Bayuk, I., Parshin, A., Miklashevskiy, D., Novikov, S. & Chekhonin, E., 2012. New methods and instruments for determination of reservoir thermal properties. Thirty-Seventh Workshop on Geothermal Reservoir Engineering, Stanford University, Stanford, California, January 30 - February 1, 2012. SGP-TR-194.

Popov, Y., Pribnow, D.F.C., Sass, J.H, Williams, C. & Burkhardt, H., 1999. Characterization of rock thermal conductivity by high-resolution optical scanning. *Geothermics*, **28**, 253-276.

Reynolds Jr., R.C. & Reynolds III, R.C. 2013. Description of Newmod II™. The calculation of one-dimensional X-ray diffraction patterns of mixed layered clay minerals. R C Reynolds III, 1526 Farlow Avenue, Crofton, MD 21114.

Rollin, K. E. 1987. Catalogue of geothermal data for the land area of the United Kingdom. Third revision: April 1987. *Investigation of the Geothermal Potential of the UK, British Geological Survey*.

Snyder, R.L. & Bish, D.L. 1989. Quantitative analysis. In: Bish, D.L., Post, J.E. (Eds), *Modern Powder Diffraction, Reviews in Mineralogy*, V. 20, Mineralogical Society of America, USA, pp. 101–144 (Chapter 5).

Vincent, C., Dashwood, B., Williams, J., Kuras, O., Kirk, K., Antcliff, P. & Barrett, M. 2019. The UK GeoEnergy Test Bed, a Unique Geoscience Research Platform. 81st EAGE Conference & Exhibition 2019, 3-6 June 2019, London, UK. pp. 5.

Warrington, G., Audley-Charles, M.G., Elliott, R.E., Evans, W.B., Ivimey-Cook, H.C., Kent, P.E., Robinson, P.L., Shotton, F.W. & Taylor, F.M. 1980. A correlation of Triassic rocks in the British Isles. *Geological Society of London, Special Report No. 13*.

Wheildon, J., Gebski, J.S. & Thomas-Betts, A. 1985. Further Investigations of the UK heat flow field (1981-1984). Investigation of the Geothermal Potential of the UK. British Geological Survey.

ACCEPTED MANUSCRIPT

List of Figures and Tables

Figure 1. Outcrop of the Mercia Mudstone Group in England and Wales. The numbered regions are as follows: 1. Wessex Basin; 2. Bristol/South Wales; 3. Worcester/Knowle Basins; 4. Needwood Basin; 5. East Midlands Shelf (South); 6. East Midlands Shelf (North); 7. Stafford Basin; 8. Cheshire Basin; 9. West Lancashire; 10. Carlisle Basin. After Howard et al. (2008). Contains 1:50,000 BGS DiGMap ©BGS UKRI and Ordnance Survey data © Crown Copyright and database rights 2020.

Figure 2. Plot of effective porosity versus measured thermal conductivity. The data display a distinctly non-linear relationship which has been approximated by a power fit of the form $Y = aX^b$.

Figure 3. Plot of calculated geometric mean thermal conductivity versus measured thermal conductivity (red symbols). The green symbols refer to the geometric mean thermal conductivity after application of a correction factor.

Figure 4. Plot of measured thermal conductivity versus the sand and clay fractions of the GTB core samples.

Table 1. Stratigraphic divisions of the Mercia Mudstone Group of England and Wales. The rock type descriptions are given in Table 2.

Table 2. Rock types of the Mercia Mudstone Group.

Table 3. Measured thermal conductivities of the MMG. Errors were calculated with Peter's formula. Values with no error are single measurements. The bracketed number is a reference to the source of the data; where (1) is Wheildon et al., (1985). Values with no reference are held by the BGS. Code is a combination of the lithostratigraphy and rock type classification.

Table 4. Mineralogical compositions of the GTB core samples (presented as volume percentages of the whole rock), effective porosity and rock classifications determined from the rock descriptions. nd = not detected.

Table 5. Measured thermal conductivities, thermal diffusivities, saturated densities and derived specific heats for the GTB core samples. nd = not determined. Thermal conductivities and diffusivities were determined from three measurements and errors have been calculated with Peter's formula.

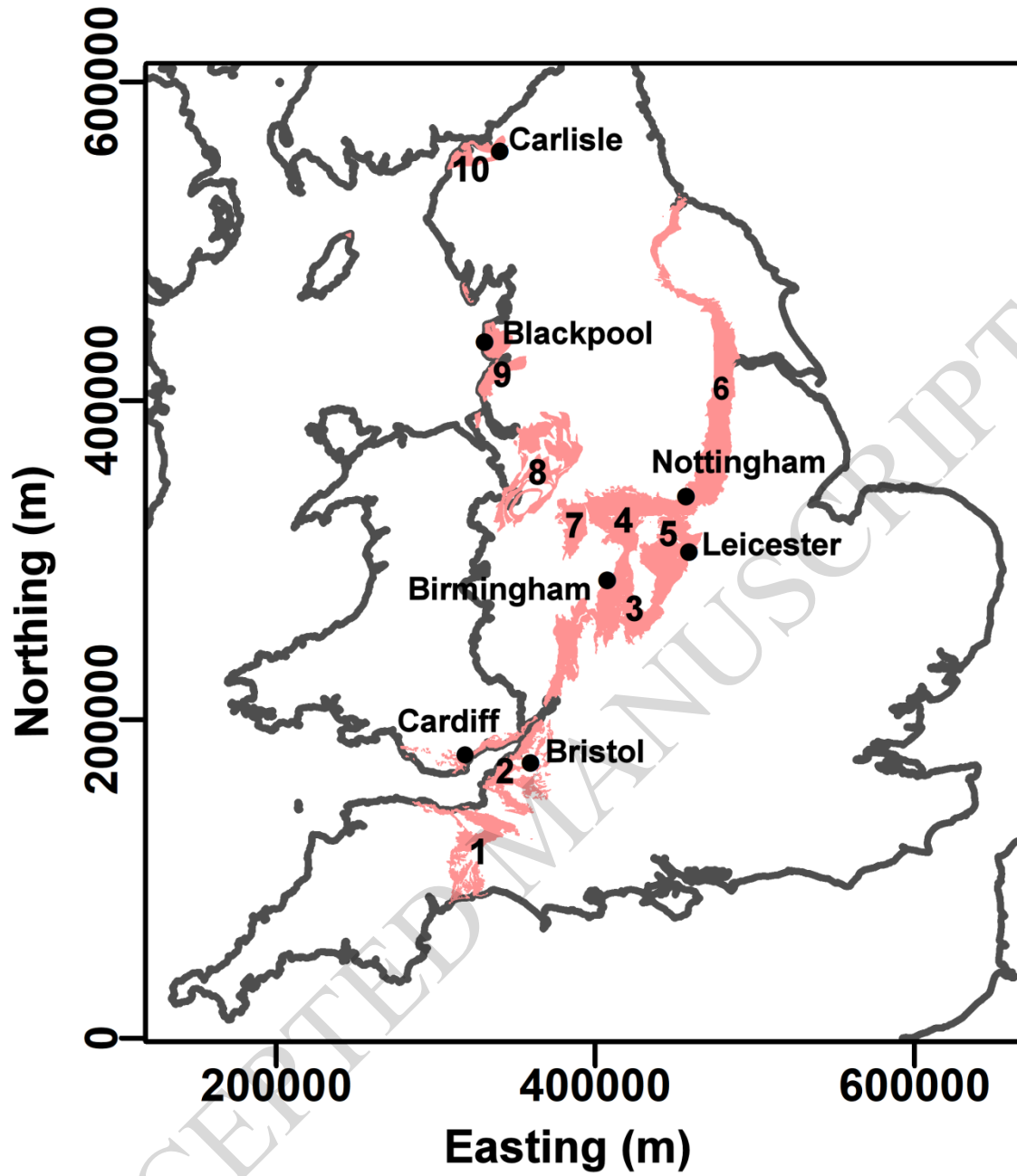
Table 6. Thermal conductivities assigned to the minerals and pore fluid in the geometric mean modelling.

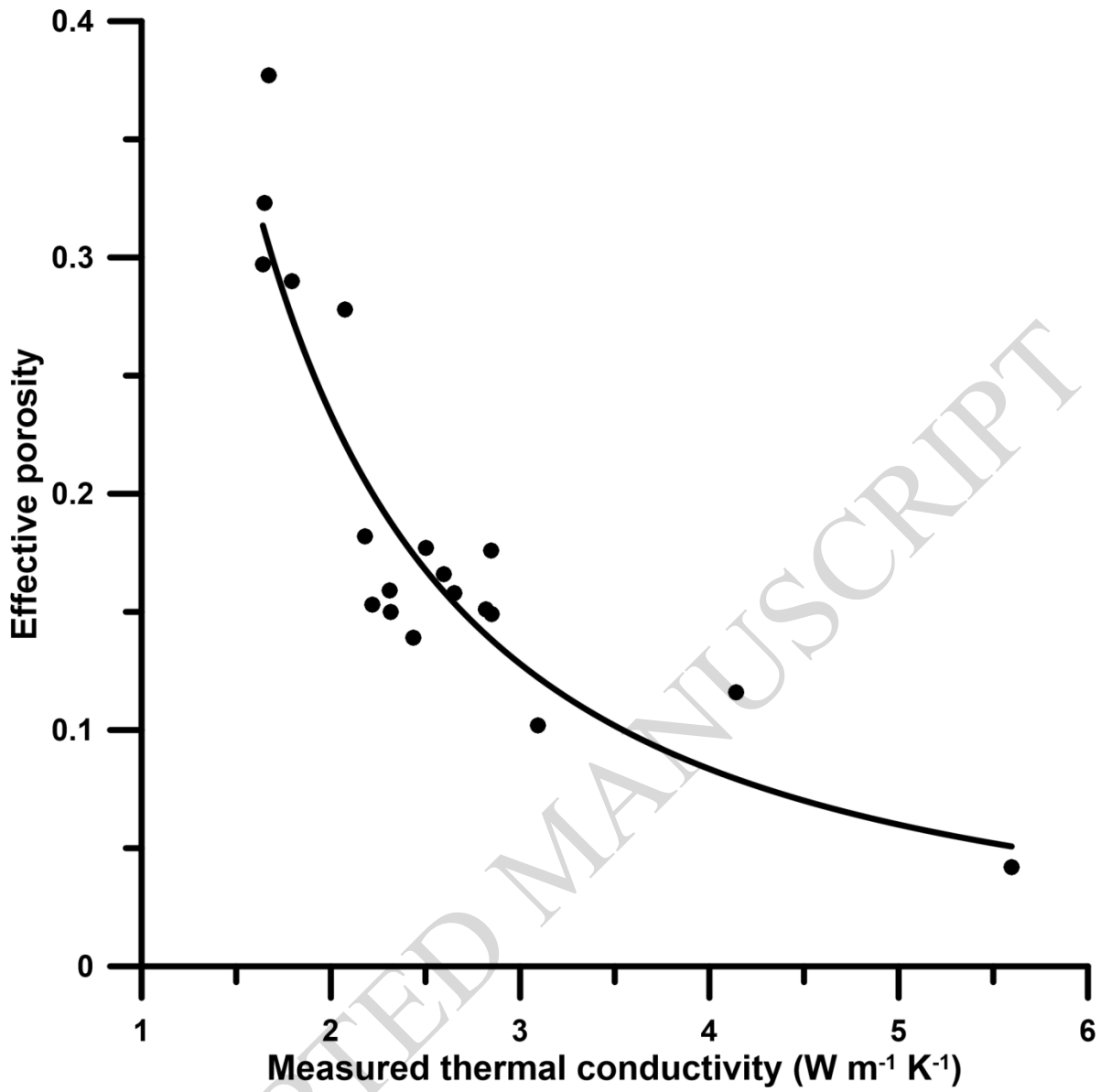
Table 7. Calculated geometric mean thermal conductivities, GSB measured saturated thermal conductivities, deviation between the measured and calculated thermal conductivities and the corrected calculated geometric mean thermal conductivities after applying a correction factor based on the lithotype. nd = not determined.

Table 8. Mineral compositions (presented as volume percentages of the whole rock) and effective porosity of the samples reported by Kemp and Hards (1999) and Armitage et al. (2013). nd = not detected.

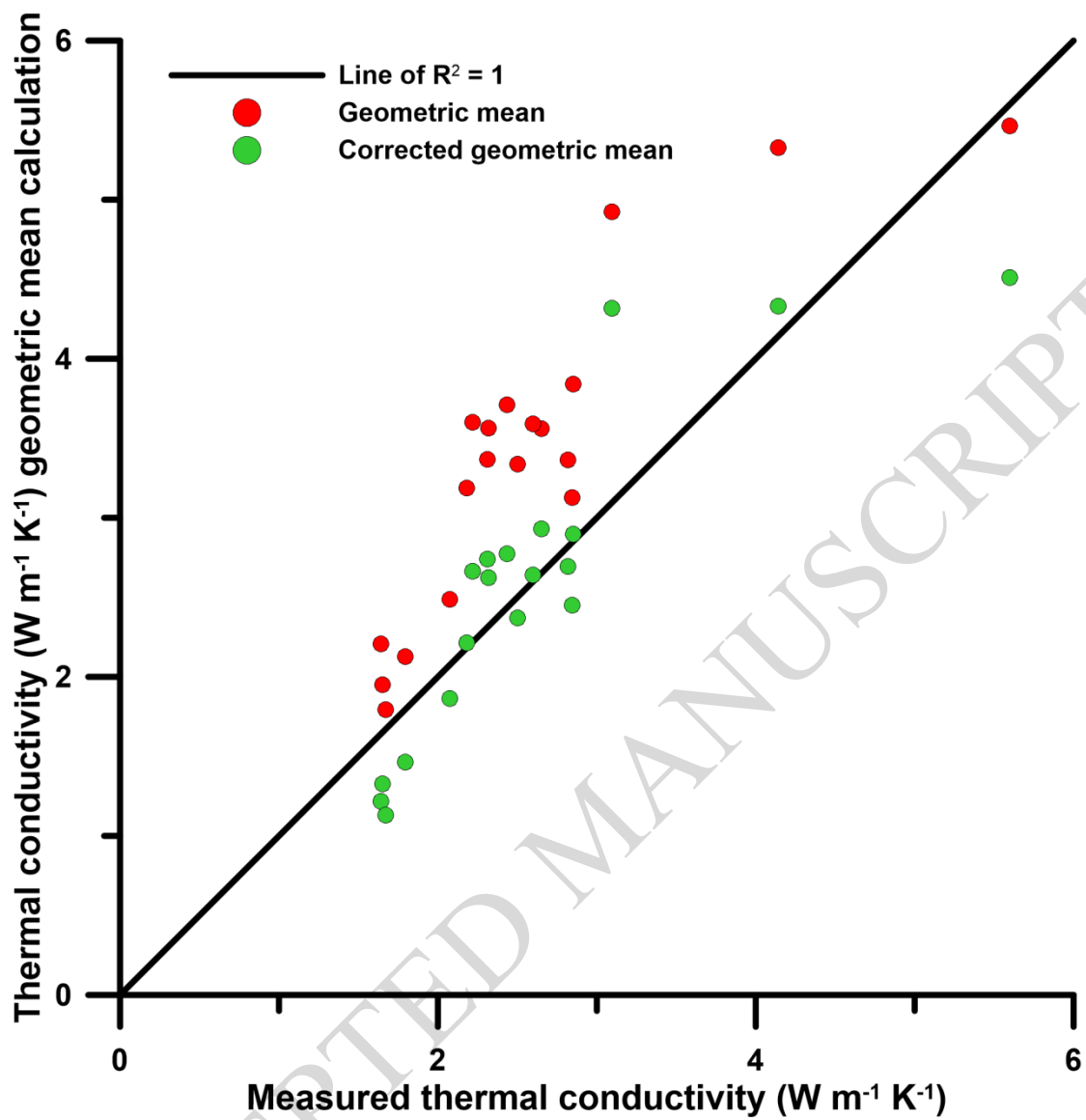
Table 9. Results of the geometric mean thermal conductivity modelling for the samples reported by Kemp and Hards (1999) and Armitage et al. (2013).

Table 10. Revised measured thermal conductivities for the East Midlands Shelf (south) MMG, incorporating the measured thermal conductivities from the GTB core.





ACCEPTED MANUSCRIPT



ACCEPTED MANUSCRIPT

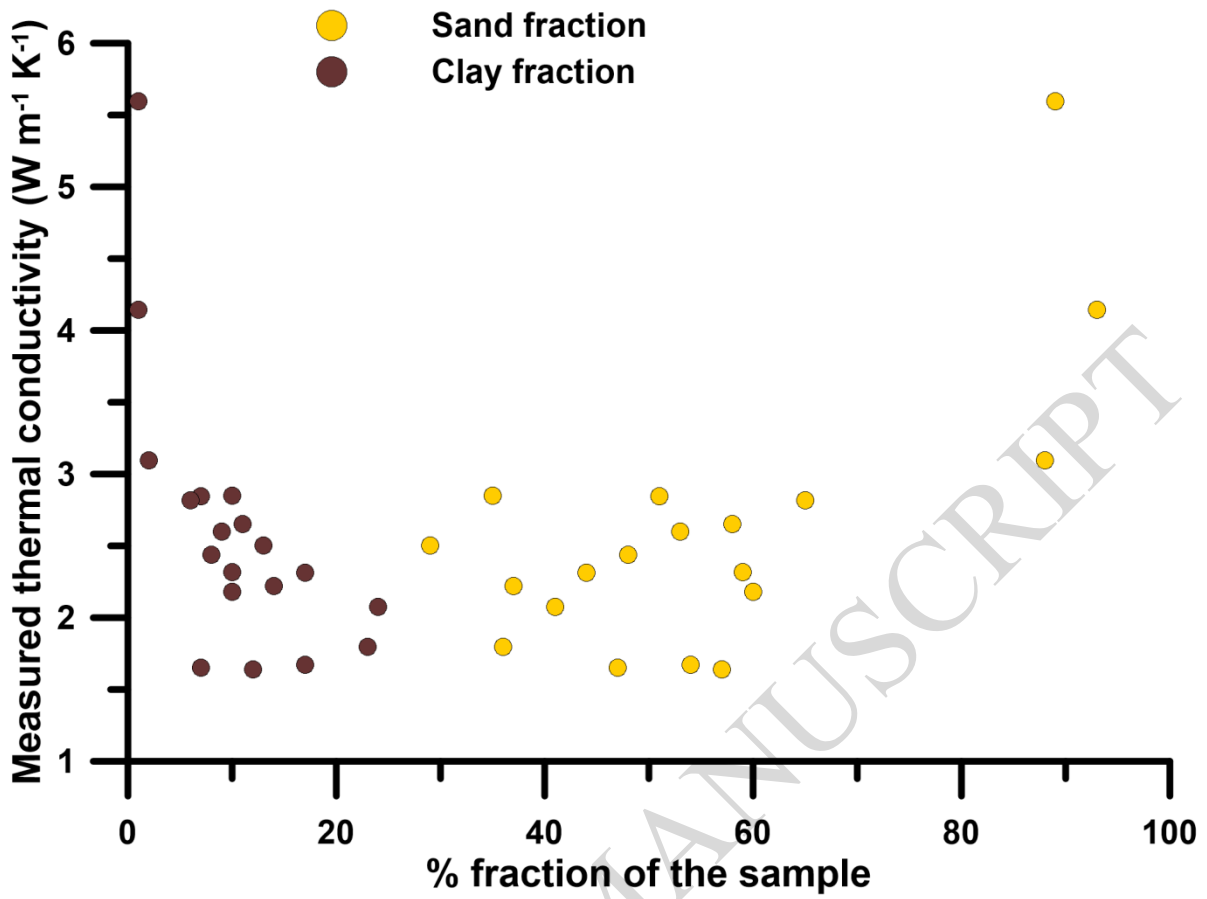


Table 1. Stratigraphic divisions of the Mercia Mudstone Group of England and Wales. The rock type descriptions are given in Table 2.

Group	Formation	Lithology	Rock types
Mercia Mudstone Group	Blue Anchor Formation (BAN)	Typically comprises pale green-grey, dolomitic silty mudstones and siltstones with thin arenaceous lenses and a few thin, commonly discontinuous beds of hard, dolomitic, pale yellowish-grey, porcellanous mudstone and siltstone. Stratified bedrock.	DSMDST, MDST, SLST, SLMDST, DOLO, GYPST
	Branscombe Mudstone Formation (BCMU)	Structureless mudstone and siltstone, red-brown with common grey-green reduction patches and spots. Gypsum/anhydrite, locally of economic importance, is common throughout in beds, nodules and veins. Sporadic thin beds of argillaceous sandstone and silty dolomite occur in the lower part of the formation. Stratified bedrock.	MDST, SLST, GYPST, SDST
	Arden Sandstone Formation (AS)	Grey, green and purple mudstones interbedded with paler grey-green to buff coloured siltstones and fine- to medium-grained, varicoloured green, brown, buff, mauve sandstone. Stratified bedrock.	MDST, SDST, SLST, CONG
	Sidmouth Mudstone Formation (SIM)	Mudstone and siltstone, red-brown with common grey-green reduction patches and spots. The mudstones are mostly structureless, with a blocky weathering habit, but intervals up to 15m thick of interlaminated mudstone and siltstone occur within parts of the formation. Heterolithic units consisting of several thin beds of grey-green dolomitic siltstone and very fine-grained sandstone, interbedded with mudstone, occur at intervals throughout the formation. Units of halite up to 400m thick are present at several stratigraphical levels in the thicker basinal sequences of the East Irish Sea, Cheshire, Staffordshire, Cleveland, Worcestershire, Somerset and Dorset, though are most prevalent towards the top. Stratified bedrock.	DSMDST, MDST, SLST, BREC, DSLST, HALI, DSDST, GYPST
	Tarporley Siltstone Formation (TPSF)	Interlaminated and interbedded siltstones, mudstones and sandstones in approximately equal proportions, trace conglomerate and limestone. Gypsum occurs sporadically in the mudstones as small nodules. Stratified bedrock.	MDST, SDST, SLST, CONG, GYPST, LMST

Table 2. Rock types of the Mercia Mudstone Group.

Code	Description	Code	Description	Code	Description
DSMDST	Dolomitic silicate-mudstone	BREC	Breccia	DOLO	Dolostone
MDS	Mudstone and sandstone	CONG	Conglomerate	GYPST	Gypsum-stone
MDSL	Mudstone, sandstone and limestone	DSDST	Dolomitic sandstone	HALI	Halite
MDSST	Muddy sandstone	DSLST	Dolomitic siltstone	LMMD	Mudmound limestone
MDST	Mudstone	SDSM	Sandstone, siltstone and mudstone	LMST	Limestone
		SDST	Sandstone		
		SLMDST	Silty mudstone		
		SLST	Siltstone		

ACCEPTED MANUSCRIPT

Table 3. Measured thermal conductivities of the MMG. Errors were calculated with Peter's formula. Values with no error are single measurements. The bracketed number is a reference to the source of the data; where (1) is Wheildon et al., (1985). Values with no reference are held by the BGS. Code is a combination of the lithostratigraphy and rock type classification.

Wessex Basin		Worcester/Knowle Basin		East Midlands Shelf (south)		Cheshire Basin	
Code	TC ($W m^{-1} K^{-1}$)	Code	TC ($W m^{-1} K^{-1}$)	Code	TC ($W m^{-1} K^{-1}$)	Code	TC ($W m^{-1} K^{-1}$)
MMG-MDST	1.95 ± 0.38						
BAN-SLMDST	2.05 (1)						
BCMU-LMMD	2.09 ± 0.16 (1)	BCMU-MDST	2.81 ± 0.26	BCMU-MDST	1.88 ± 0.19		
BCMU-MDSL	2.34 ± 0.1 (1)			BCMU-SLST	2.12		
BCMU-SLMDST	1.96 ± 0.41 (1)						
		AS-SDST	3.17	AS-SDST	2.94		
SIM-SLMDST	1.72 (1)	SIM-MDSD	2.63 (1)	SIM-DSDST	2.76	SIM-MDST	1.89 ± 0.06 (1)
		SIM-MDST	2.05 ± 0.1 (1)	SIM-MDST	1.71 ± 0.14	SIM-SLMDST	1.69 ± 0.12 (1)
		SIM-SLMDST	1.94 ± 0.12 (1)	SIM-SDST	4.43		
		SIM-SLST	2.19 ± 0.31 (1)	SIM-SLST	2.40 ± 0.41		
				TPSF-SDST	2.70 ± 0.37		

Table 4. Mineralogical compositions of the GTB core samples (presented as volume percentages of the whole rock), effective porosity and rock classifications determined from the rock descriptions. nd = not detected.

SSK Number	Depth (m)	Strata	Volume % of whole rock													
			Quartz	Plagioclase	K-feldspar	Mica (excl illite)	Illite	Smectite	Chlorite (inc corrensite)	Calcite	Dolomite	Hematite	Gypsum	Anhydrite	Effective porosity	Rock type classification
109105	9.3-9.4	Arden Sst Fm	17.8	0.9	<0.5	3.7	4.2	4.2	0.8	1.1	8.3	<0.5	29.1	nd	29.7	SDST
109102	14.4-14.5		9.5	1.2	<0.5	3.6	3.6	7.6	1.7	0.7	9.6	<0.5	24.2	nd	37.7	MDSST
109103	21.7-21.8	Sidmouth Mdst Fm	18.0	2.3	<0.5	22.9	3.6	nd	2.9	nd	4.3	nd	13.3	nd	32.3	MDST
109104	30.3-30.5		72.5	1.8	<0.5	7.9	0.9	nd	0.7	nd	3.2	<0.5	2.5	nd	10.2	MDSST
109080	37.1-37.5		21.5	2.8	1.6	6.9	6.8	14.7	5.6	nd	6.7	<0.5	4.1	nd	29.0	MDST
109081	45.7-46.0		35.2	1.9	1.9	5.4	12.1	nd	7.6	nd	2.4	<0.5	5.6	nd	27.8	MDSST
109082	54.6-54.7		60.8	nd	5.4	1.4	<0.5	nd	<0.5	nd	3.3	nd	3.7	20.5	4.2	SDST
109083	65.3-65.4		43.2	3.8	5.7	7.4	7.1	nd	1.5	nd	16.3	nd	nd	nd	15.0	SDST
109084	68.0-68.1		8.1	0.6	3.9	2.9	4.5	nd	<0.5	nd	46.4	nd	15.6	nd	17.6	MDSST
109085	76.8-77.1		13.4	<0.5	5.4	3.9	3.7	nd	1.9	nd	43.7	nd	12.6	nd	15.1	MDSST
109086	85.6-85.7		37.1	<0.5	8.5	4.5	7.3	nd	1.4	nd	23.4	<0.5	1.8	nd	15.8	MDST
109087	93.9-94.0		30.9	<0.5	7.1	6.0	6.1	nd	1.8	nd	19.9	<0.5	9.8	nd	18.2	SDST
109088	100.7-100.8		26.8	<0.5	5.6	3.6	7.8	nd	2.0	nd	32.5	<0.5	3.5	nd	17.7	SDST
109089	108.7-108.8		41.4	0.8	5.2	6.0	7.7	nd	1.4	nd	18.0	<0.5	2.1	nd	17.1	SDSM
109096	116.4-116.5		45.6	<0.5	6.4	9.8	4.7	nd	4.6	nd	12.7	nd	2.0	nd	13.9	SDST
109097	124.4-124.6		54.2	0.8	6.4	6.4	6.6	nd	1.0	nd	7.9	<0.5	1.8	nd	14.9	SDSM
109098	131.9-132.0		Tarpotley Slst Fm	47.7	0.7	3.7	7.8	6.3	nd	0.7	nd	10.6	<0.5	5.7	nd	16.6
109099	140.4-140.6	39.9		0.7	7.1	6.9	12.8	nd	0.7	nd	15.6	<0.5	<0.5	nd	15.9	MDST
109100	148.3-148.4	80.5		nd	0.5	nd	0.6	<0.5	nd	nd	<0.5	<0.5	6.2	nd	11.6	SDST
109101	155.8-156.0	47.9		<0.5	5.2	7.9	10.3	nd	1.5	nd	10.9	<0.5	0.7	nd	15.3	SLST

Table 5. Measured thermal conductivities, thermal diffusivities, saturated densities and derived specific heats for the GTB core samples. nd = not determined. Thermal conductivities and diffusivities were determined from three measurements and errors have been calculated with Peter's formula.

SSK number	Strat	Thermal conductivity (W m ⁻¹ K ⁻¹)	Thermal diffusivity (x10 ⁻⁶ m ² s ⁻¹)	Saturated density (kg m ⁻³)	Specific heat capacity by mass (J K ⁻¹ kg ⁻¹)	Specific heat capacity by volume (MJ m ⁻³ K ⁻¹)
109105	Arden Sst Fm	1.64 ± 0.01	0.64 ± 0.03	2315	1109	2.57
109102		1.67 ± 0.02	0.79 ± 0.08	2143	993	2.13
109103	Sidmouth Mdst Fm	1.65 ± 0.03	0.63 ± 0.05	2227	1179	2.63
109104		3.10 ± 0.05	1.43 ± 0.07	2497	867	2.17
109080		1.79 ± 0.02	0.64 ± 0.01	2236	1254	2.80
109081		2.07 ± 0.01	0.65 ± 0.07	2235	1426	3.19
109082		5.60 ± 0.15	3.07 ± 0.29	2653	688	1.82
109083		2.32 ± 0.01	1.47 ± 0.05	2454	643	1.58
109084		2.85 ± 0.03	1.12 ± 0.07	2499	1019	2.55
109085		2.82 ± 0.03	1.70 ± 0.05	2473	669	1.65
109086		2.65 ± 0.02	1.16 ± 0.01	2443	940	2.30
109087		2.18 ± 0.03	0.95 ± 0.02	2575	891	2.29
109088		2.50 ± 0.01	1.48 ± 0.15	2643	642	1.70
109089		nd	nd	nd	nd	nd
109096		2.44 ± 0.04	1.06 ± 0.03	2530	910	2.30
109097		2.85 ± 0.03	1.31 ± 0.16	2437	894	2.18
109098	Tarporley Sst Fm	2.60 ± 0.04	0.96 ± 0.09	2610	1034	2.70
109099		2.31 ± 0.33	1.56 ± 0.18	2636	563	1.48
109100		4.14 ± 0.02	2.11 ± 0.09	2585	760	1.96
109101		2.22 ± 0.02	1.03 ± 0.0	2474	871	2.16

Table 6. Thermal conductivities assigned to the minerals and pore fluid in the geometric mean modelling.

Model component	Thermal conductivity (W m ⁻¹ K ⁻¹)	Reference
Hematite	11.28	Clouser and Huenges (1995)
Quartz	7.69	Clouser and Huenges (1995)
Dolomite	5.51	Clouser and Huenges (1995)
Anhydrite	4.76	Horai (1971)
Calcite	3.59	Clouser and Huenges (1995)
Chlorite	3.26	Brigaud and Vasseur (1989)
Gypsum	2.9	Brigaud and Vasseur (1989)
K-feldspar	2.45	Horai (1971)
Mica (excl. Illite)	2.2	Horai (1971)
Smectite	1.88	Brigaud and Vasseur (1989)
Illite	1.85	Brigaud and Vasseur (1989)
Plagioclase	1.84	Horai (1971)
Water	0.6	Ozbek and Phillips (1979)

ACCEPTED MANUSCRIPT

Table 7. Calculated geometric mean thermal conductivities, GSB measured saturated thermal conductivities, deviation between the measured and calculated thermal conductivities and the corrected calculated geometric mean thermal conductivities after applying a correction factor based on the lithotype. nd = not determined.

SSK number	Strat	Geometric mean thermal conductivity ($\text{W m}^{-1} \text{K}^{-1}$)	Measured thermal conductivity ($\text{W m}^{-1} \text{K}^{-1}$)	Deviation measured to calculated thermal conductivity ($\text{W m}^{-1} \text{K}^{-1}$)	Lithotype	Corrected geometric mean thermal conductivity ($\text{W m}^{-1} \text{K}^{-1}$)
109105	Arden	2.18	1.64 ± 0.01	-0.53	Sandstone	1.22
109102	Sst Fm	1.77	1.67 ± 0.02	-0.09	Mudstone	1.13
109103	Sidmouth Mdst Fm	1.96	1.65 ± 0.03	-0.31	Mudstone	1.33
109104		4.95	3.10 ± 0.05	-1.86	Mudstone	4.32
109080		2.10	1.79 ± 0.02	-0.30	Mudstone	1.46
109081		2.50	2.07 ± 0.01	-0.42	Mudstone	1.86
109082		5.47	5.60 ± 0.15	0.13	Sandstone	4.51
109083		3.58	2.32 ± 0.01	-1.27	Sandstone	2.62
109084		3.09	2.85 ± 0.03	-0.24	Mudstone	2.45
109085		3.33	2.82 ± 0.03	-0.51	Mudstone	2.69
109086		3.56	2.65 ± 0.02	-0.91	Mudstone	2.93
109087		3.17	2.18 ± 0.03	-0.99	Sandstone	2.21
109088		3.33	2.50 ± 0.01	-0.83	Sandstone	2.37
109089		nd	nd	nd	Sandstone	nd
109096		3.73	2.44 ± 0.04	-1.30	Sandstone	2.77
109097		3.86	2.85 ± 0.03	-1.01	Sandstone	2.90
109098		Tarpoley Slst Fm	3.60	2.60 ± 0.04	-1.00	Sandstone
109099	3.38		2.31 ± 0.33	-1.06	Mudstone	2.74
109100	5.29		4.14 ± 0.02	-1.15	Sandstone	4.33
109101	3.62		2.22 ± 0.02	-1.40	Sandstone	2.66

Table 8. Mineral compositions (presented as volume percentages of the whole rock) and effective porosity of the samples reported by Kemp and Hards (1999) and Armitage et al. (2013). nd = not detected.

Sample Number	Depth (m)	Strata	Volume % of whole rock											
			Quartz	Plagioclase	K-feldspar	Mica	Illite	Smectite	Chlorite	Calcite	Dolomite	Hematite	Gypsum	Effective porosity
		Sidmouth Mdst Fm	Kemp and Hards (1999)											
Borehole 2/2	8.0		21.7	0.9	7.5	7.5		17.7	0.9	13.2	9.3	0.5	nd	21.0
Borehole 2/6	8.5-10.0		30.1	1.7	8.0	6.3		11.9	0.8	16.8	3.2	0.0	nd	21.0
Borehole 2/8	8.0		32.8	1.8	8.3	8.2		13.3	0.8	3.5	9.9	0.5	nd	21.0
Borehole 2/10	8.25-9.0		31.7	2.6	8.9	7.1		13.8	0.8	0.8	12.8	0.4	nd	21.0
Borehole 2/13	9.1-10.3		15.0	0.8	8.6	5.4		26.9	0.8	15.5	5.5	0.4	nd	21.0
			Armitage et al. (2013)											
M1	300.0		29.4	1.8	14.7		36.9		5.3	3.1	1.3	nd	0.0	7.4
M2	300.4		39.6	1.5	10.3		14.0		3.9	0.4	7.4	nd	12.4	10.3
M3	301.5		29.1	2.1	10.4		16.0		3.7	0.2	11.1	nd	16.9	10.7
M4	302.6		39.7	0.5	7.0		30.7		4.2	0.2	8.4	nd	0.1	9.1
M5	307.5		43.1	0.1	7.9		33.5		4.4	0.1	1.3	nd	0.0	9.7
M6	309.3		59.3	0.9	5.9		3.8		1.4	0.9	3.2	nd	15.1	9.5

ACCEPTED MANUSCRIPT

Table 9. Results of the geometric mean thermal conductivity modelling for the samples reported by Kemp and Hards (1999) and Armitage et al. (2013).

Sample number	Strat	Rock type	Geometric mean thermal conductivity (W m ⁻¹ K ⁻¹)	Correction factor applied	Corrected geometric mean thermal conductivity (W m ⁻¹ K ⁻¹)	
Kemp and Hards (1999)						
Borehole 2/2	Sidmouth Mdst Fm	MDST	2.49	-0.63	1.86	
Borehole 2/6		SDSM	2.67	-0.96	1.71	
Borehole 2/8		MDST	2.76	-0.63	2.13	
Borehole 2/10		MDST	2.76	-0.63	2.13	
Borehole 2/13		SLMDST	2.21	-0.63	1.57	
Armitage et al. (2013)						
M1		SLMDST	2.82	-0.63	2.19	
M2		SLST	3.13	-0.96	2.17	
M3		SLMDST	2.74	-0.96	1.78	
M4		SLMDST	3.33	-0.63	2.70	
M5	SLMDST	3.22	-0.96	2.26		
M6	SDST	3.88	-0.96	2.92		

ACCEPTED MANUSCRIPT

Table 10. Revised measured thermal conductivities for the East Midlands Shelf (south) MMG, incorporating the measured thermal conductivities from the GTB core.

East Midlands Shelf (south)	
Code	TC ($\text{W m}^{-1} \text{K}^{-1}$)
BCMU-MDST	1.88 ± 0.19
BCMU-SLST	2.12
AS-MDSST	1.67
AS-SDST	2.3 ± 0.81
SIM-DSDST	2.76
SIM-MDSST	2.71 ± 0.23
SIM-MDST	1.81 ± 0.39
SIM-SDSM	2.85
SIM-SDST	3.24 ± 0.66
SIM-SLST	2.40 ± 0.41
TPSF-MDST	2.31
TPSF-SDST	2.99 ± 0.47
TPSF-SLST	2.41 ± 0.24

ACCEPTED MANUSCRIPT